

## Performance Comparison of Si, $\text{In}_{0.53}\text{Ga}_{0.47}\text{As}$ and GaSb 10-nm Double Gate nMOSFETs by Deterministically Solving Time Dependent BTE

Shaoyan Di<sup>1</sup>, Lei Shen<sup>1</sup>, Zhiyuan Lun<sup>1</sup>, Pengying Chang<sup>1</sup>, Kai Zhao<sup>3,1,\*</sup>, Tiao Lu<sup>2</sup>, Gang Du<sup>1</sup>, Xiaoyan Liu<sup>1,\*</sup>

<sup>1</sup>Institute of Microelectronics, Peking University, 100871 Beijing, China

<sup>2</sup>CAPT, HEDPS, IFSA Collaborative Innovation Center of MoE, LMAM & School of Mathematical Sciences, Peking University, Beijing, China.

<sup>3</sup>School of Information and Communication, Beijing Information Science and Technology University, Beijing 100101, China

### Abstract

The performance of 10-nm double gate nMOSFETs with Si,  $\text{In}_{0.53}\text{Ga}_{0.47}\text{As}$  and GaSb are compared by using a deterministic Boltzmann transport equation (BTE) solver. The results show that the GaSb device exhibits the highest on-current while  $\text{In}_{0.53}\text{Ga}_{0.47}\text{As}$  device has the highest injection velocity and ballistic ratio but suffers from the density of state (DoS) bottle neck seriously.

### 1. Introduction

III-V material is becoming a strong candidate to substitute Si for devices of next generation [1] due to its high mobility [2]. However, the advantage may be compensated by its small DoS [3]. Recent works show that GaSb devices with a surface orientation of (111) can get relatively higher DoS without a big degradation of injection velocity [4]. Many comparison works have done among various III-V material and Si devices [5, 6] but some details during the carrier transport are still unclear. In this work 10-nm double gate devices made of Si, InGaAs and GaSb are compared by deterministically solving time dependent BTE.

### 2. Simulation method and device structure

A deterministic BTE solver [7-9] is employed in this work. The time dependent BTE is solved by a positive and flux conservative (PFC) method [7]. Besides, a self-consistent Schrödinger-Poisson iteration is involved to consider the quantum confinement.

10-nm double gate nMOSFETs (shown in Fig. 1) with Si, InGaAs and GaSb are compared in this paper. The Si and InGaAs devices have the surface orientation of (100) while the GaSb device is with the (111) surface orientation because the (111) GaSb device exhibits better performance [5]. Structure parameters of devices made of different material are set mainly according to ITRS2013[10] and listed in Table I.

We have involved the intra-valley acoustic (AP) and optical phonon (OP) scattering, inter-valley optical phonon scattering (f-type, g-type for Si and  $\Gamma$ -L, L-L for III-V material), and surface roughness scattering (SR). For III-V devices, the polar optical phonon scattering (POP) is also considered. The band and scattering parameters are extracted from [11-14]. Besides, the Pauli's exclusion principle is also involved.

### 3. Results and discussions

The  $I_D$ - $V_G$  curves of the simulated devices are shown in Fig. 2. The off-current is tuned to be  $10^{-3}$  A/cm by shifting the work function. The GaSb device shows the highest on current. While a better SS of 63mV/dec is exhibited by Si devices because of its thinner body and smaller dielectric constant [6]. The SS of InGaAs and GaSb devices are 68mV/dec and 65mV/dec, respectively.

Fig. 3 shows the subband profiles of 3 types of devices. We have considered 4 groups of 2-fold degenerate unprimed subbands and the lowest 4-fold primed subbands for Si. As for InGaAs, the lowest subband of  $\Gamma$  valley and 2 groups of 4-fold degenerate subband of L valleys are involved. While for the GaSb devices with (111) surface orientation, one of the original 4-fold degenerate L valleys, which is projected to the  $\Gamma$  point after the confinement, become different with other 3 valleys. In such a circumstance we have considered 7 subbands of the non-degenerate L valley and 2 subbands for the 3-fold L valleys. By contrast we can see that the subbands of InGaAs have to be lower than other cases to get enough electrons due to its smaller DoS, which made the device suffer from the DoS bottle neck seriously. We have calculated the quantum capacitance ( $C_Q = \partial qN / \partial(-U_{scf}/q)$ ) [15] of all kinds of devices and illustrated in Fig. 4. Si and GaSb devices have a much higher quantum capacitance than  $C_{ox}$  ( $0.0345 \text{ F/m}^2$ ). However, the  $C_Q$  of the InGaAs device is only 1.86 times of  $C_{ox}$ , which degraded the gate capacitance ( $C_G$ ) significantly.

Fig. 5 shows the carrier density and injection velocity at the virtual source [16]. Despite the InGaAs device shows the lowest carrier density due to the DoS bottle neck, the injection velocity is as big as  $6 \times 10^7 \text{ cm/s}$ , which is the highest among the simulated devices because more than 90% of the carriers populate in the subband with a much smaller transport effective mass ( $m^* = 0.048m_0$ ), as shown in Fig. 6.

The scattering spectrum is shown in Fig. 7. The scattering rate of III-V material is much smaller than Si. Especially for InGaAs, the scattering rate is almost 2 orders smaller than Si in low kinetic energy region. The electron's kinetic energy distribution is illustrated in Fig. 8. At source and the virtual source, the electrons are within equilibrium state and accelerated to much higher energy state after the transport process. However, the energy dissipation during the transport is different. The magnitude of energy dissipation for Si is the biggest due to its larger scattering rate. While for InGaAs, almost no dissipation can be observed. Fig. 9 shows the currents under ballistic and scattering conditions and the ballistic ratio ( $B = I_{scat} / I_{ball}$ ) is also calculated. The ballistic ratio of InGaAs is 94.7%, indicating that the carriers transport through the channel almost in a ballistic fashion. While for Si, the ballistic ratio is much lower due to the stronger scattering mechanisms.

### 4. Conclusions

We have compared the performance of 10-nm (100) Si, (100)  $\text{In}_{0.53}\text{Ga}_{0.47}\text{As}$  and (111) GaSb double gate nMOSFETs. It shows that the GaSb device exhibits the best drive current and device made of InGaAs shows the highest injection velocity and ballistic ratio but suffers from the DoS bottle neck more seriously.

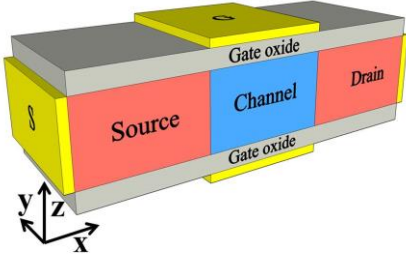


Fig. 1. The schematic structure of the simulated double gate devices.

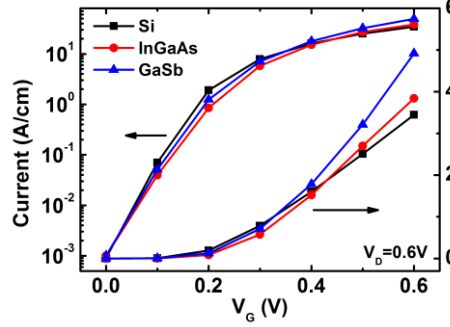


Fig. 2. The  $I_D$ - $V_G$  curves of the simulated devices with  $V_D=0.6V$ .

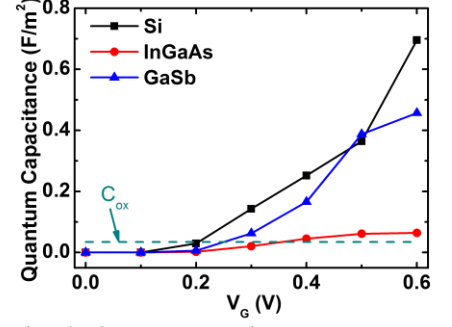


Fig. 4. Quantum capacitance versus gate voltage.

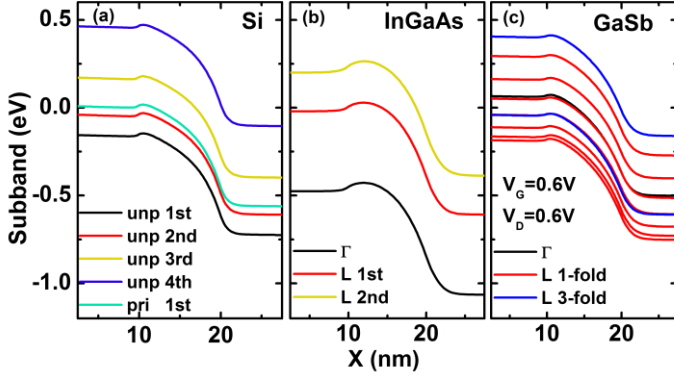


Fig. 3. The subband profiles of devices made of various material.

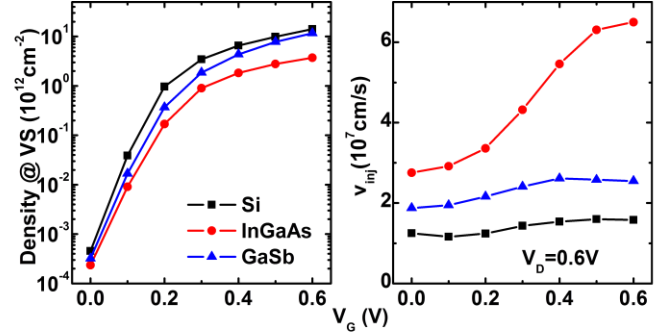


Fig. 5. (a) Carrier density and (b) injection velocity versus gate voltage at the virtual source with  $V_D=0.6V$ .

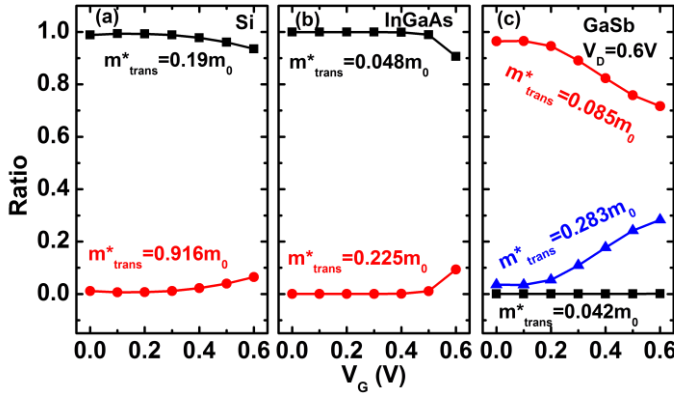


Fig. 6. The ratio of electrons in subbands with different transport effective masses at the virtual source.

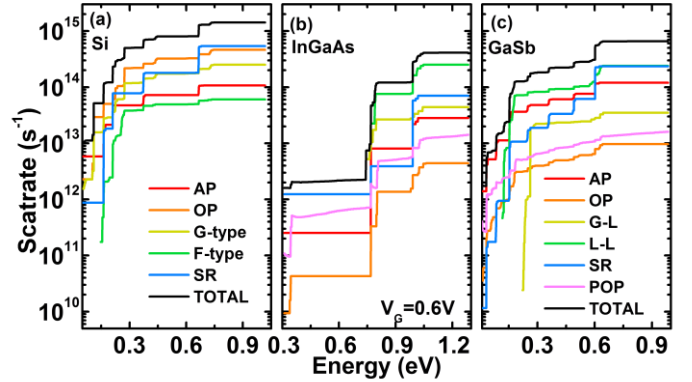


Fig. 7. Electron scattering spectrums of devices made of various material.

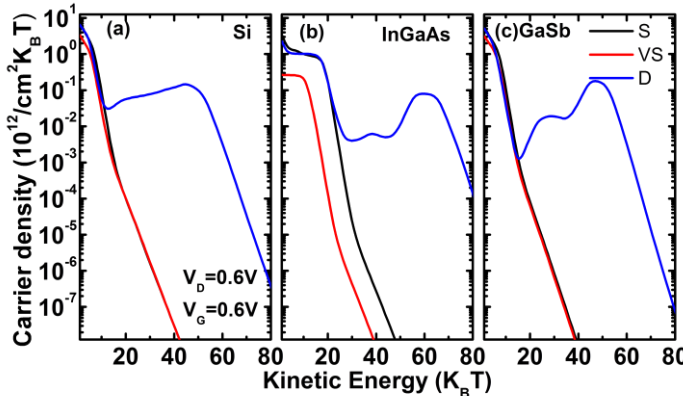


Fig. 8. Kinetic energy distribution at source, virtual source and drain.

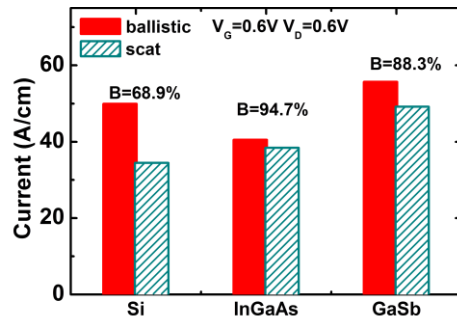


Fig. 9. Comparison of currents w/wo scattering. The ballistic ratio  $B$  is also calculated.

## Acknowledgements

This work is supported by the National Natural Science Foundation of China under Grant 91434201 and 61421005.

## References

- [1] S. Takagi, et al. ESSDERC, 2015. [2] K. Kalna, et al. ESSDERC, 2005. [3] P. M. Solomon, et al. IEDM, 2001. [4] M. Rodwell, et al. proc. DRC, 2010. [5] R. Kim, et al. EDL, **32**(2011), 746. [6] M. Luisier, EDL, **32**(2011), 1686. [7] T. Lu, et al. Commun. Comput. Phys., **10**(2011). [8] S. Di, et al. J. Comp. Elec., 2016. [9] S. Di, et al. VLSI-TSA, 2016. [10] www.itrs.net. [11] M. V. Fischetti, TED, **38**(1991), 634. [12] P. Damayanthi, et al., J. App. Phys., **86**(1999), 5060. [13] J. G. Ruch, App. Phys. Lett. **20**(1972), 246. [14] P. S. Dutta, et al. J. App. Phys. **81**(1997), 5821. [15] A. Rahman, et al., TED, **50**(2003), 1853. [16] M. S. Lundstrom, EDL, **18**(1997), 361.

Parameters	Si	InGaAs	GaSb
Surface orientation	(100)	(100)	(111)
Channel length	10nm	10nm	10nm
S/D length	10nm	10nm	10nm
EOT	1nm	1nm	1nm
Film thickness	3nm	5nm	5nm
Channel doping	$10^{17} \text{cm}^{-3}$	$10^{17} \text{cm}^{-3}$	$10^{17} \text{cm}^{-3}$
S/D doping	$10^{20} \text{cm}^{-3}$	$5 \times 10^{19} \text{cm}^{-3}$	$5 \times 10^{19} \text{cm}^{-3}$